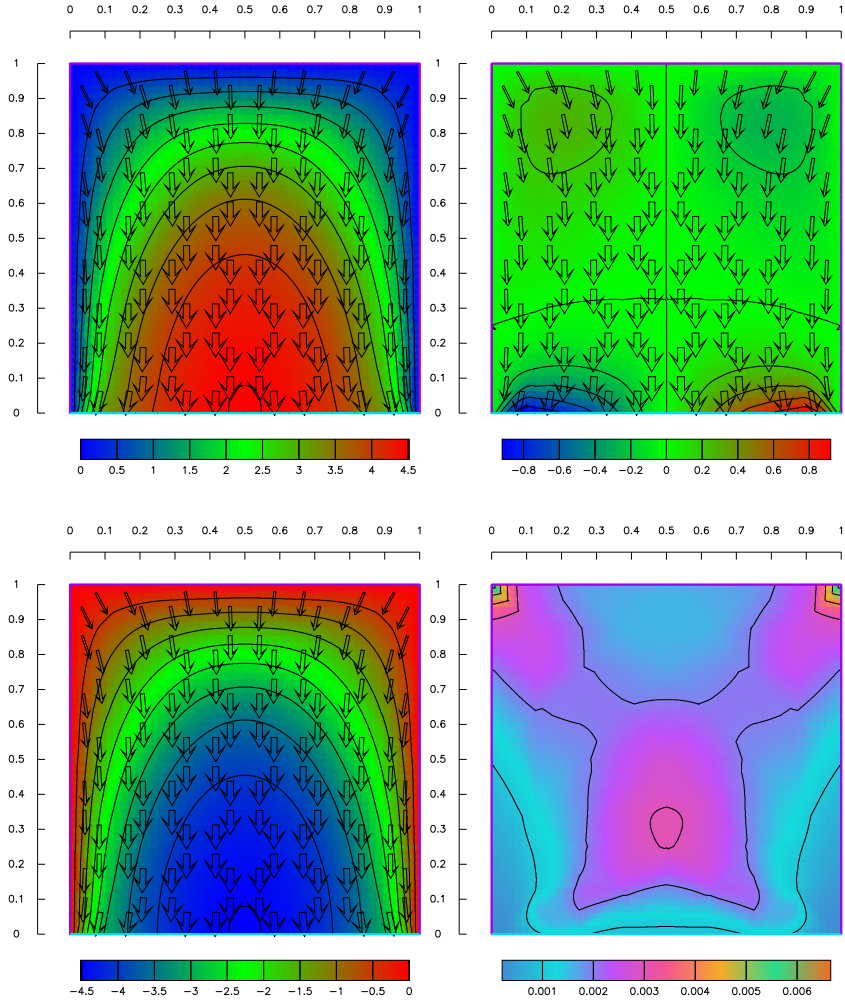

Figure II.19.: v, v_x, v_y and $\bar{\nu}$ (from left to right, from top to bottom) for the ice-ramp setup. 40 iterations, $a_{\max} = 0.01$.

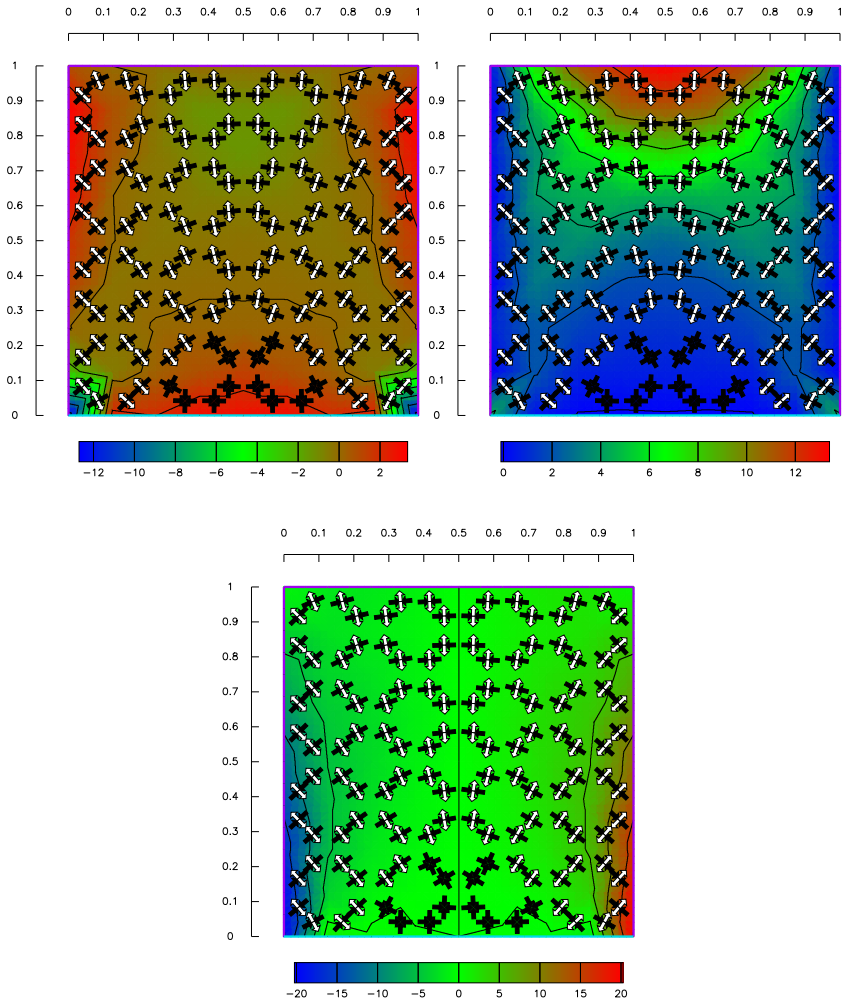

Figure II.20.: The strain-rate tensor components D_x, D_y and D_{xy} (from left to right, from top to bottom) for the ice-ramp setup. 40 iterations, $a_{\max} = 0.01$.

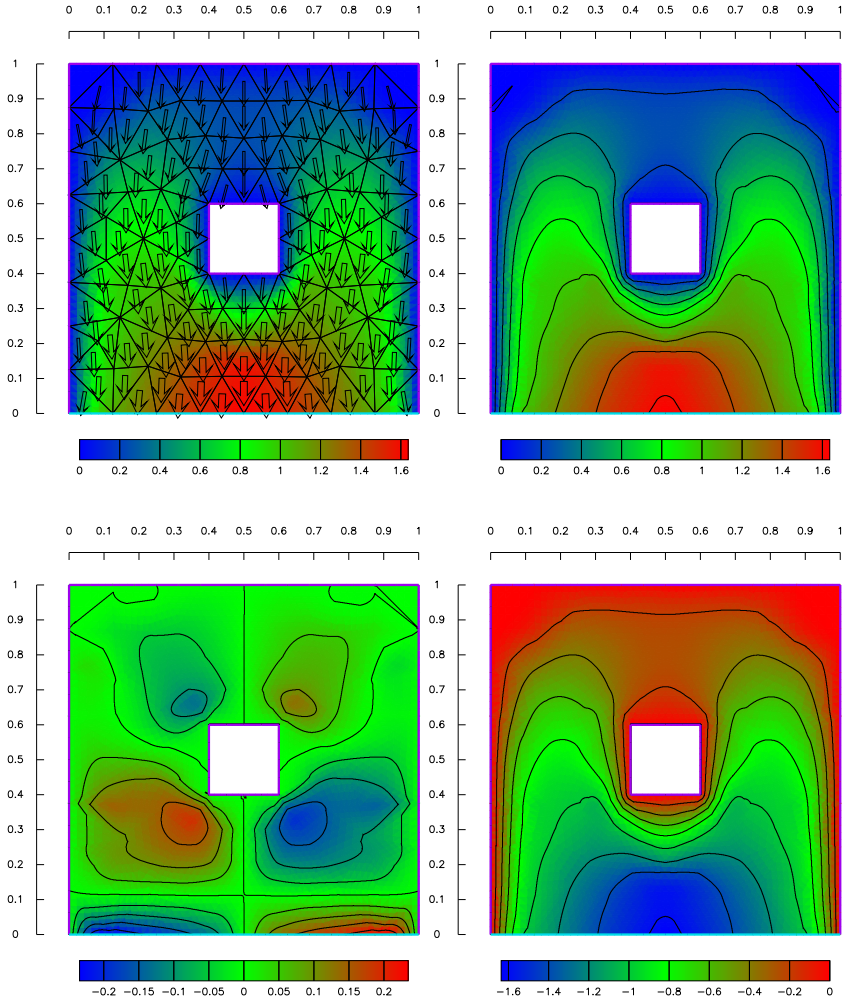

Figure II.21.: The velocity field together with the grid, v, v_x, and v_y (from left to right, from top to bottom) for the ice-rise setup. 60 iterations, $a_{\max} = 0.01$.

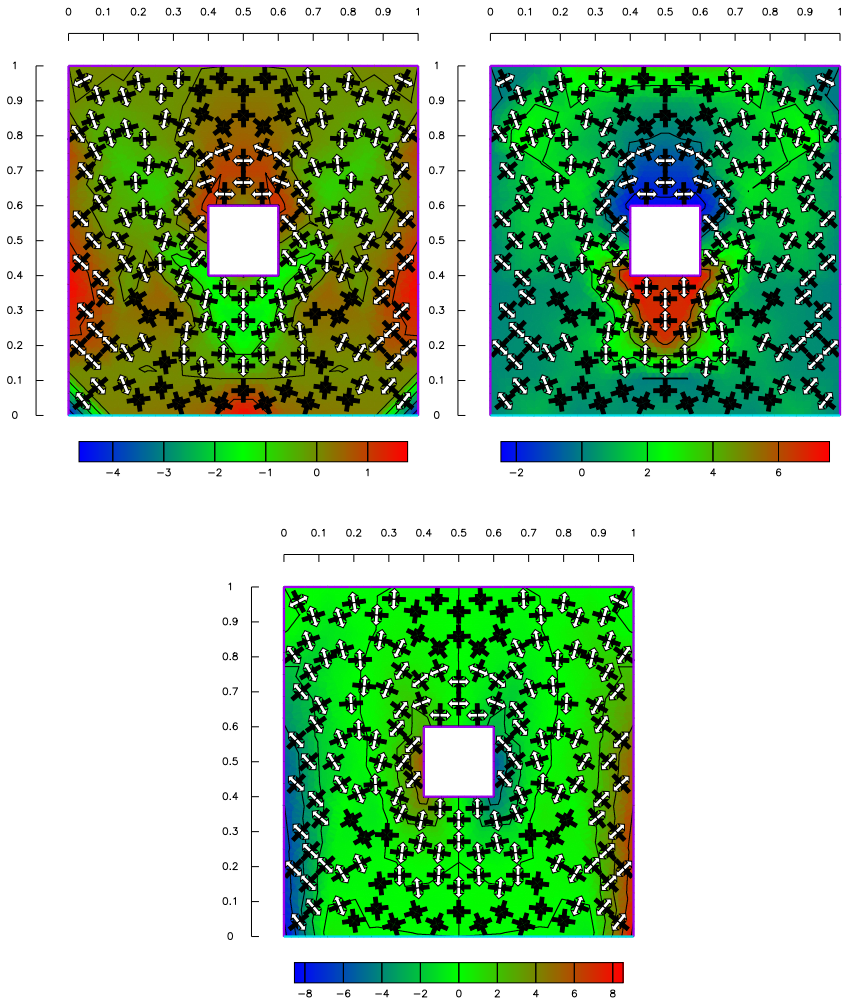

Figure II.22.: The strain-rate tensor components D_x, D_y and D_{xy} (from left to right, from top to bottom) for the ice-rise setup. 60 iterations, $a_{\max} = 0.01$.

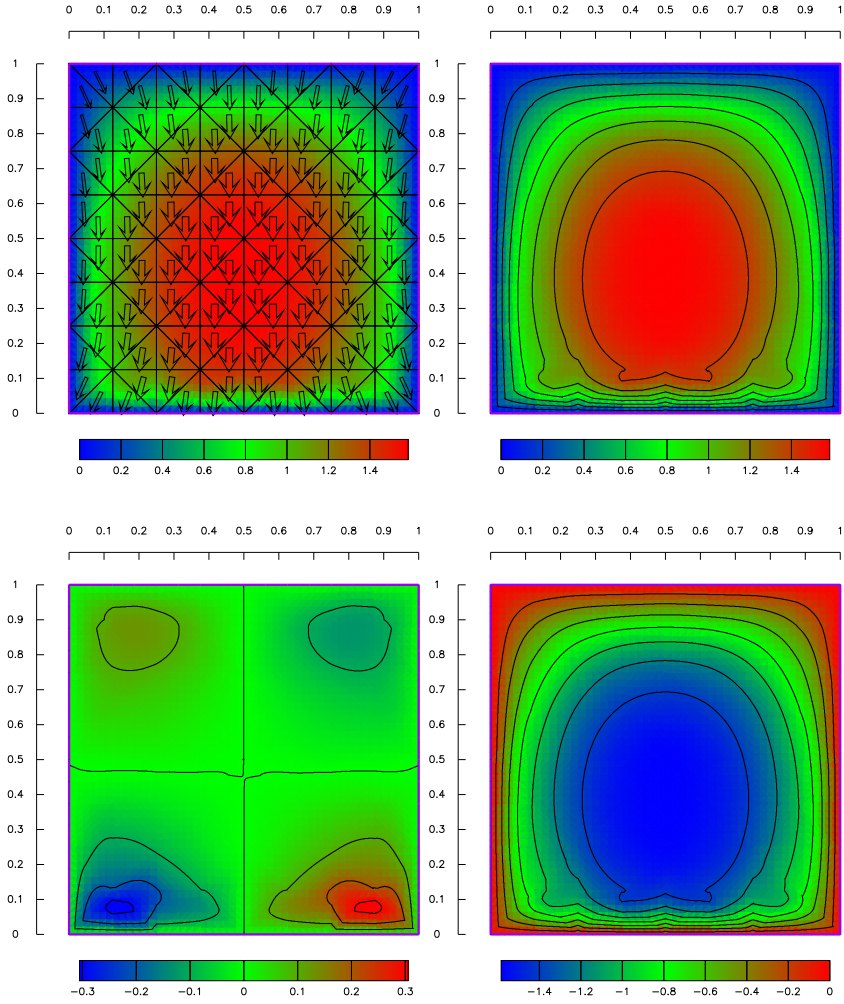

Figure II.23.: The velocity field together with the grid, v, v_x, and v_y (from left to right, from top to bottom) for the "locked up" ice ramp. 40 iterations, $a_{\max} = 0.01$.

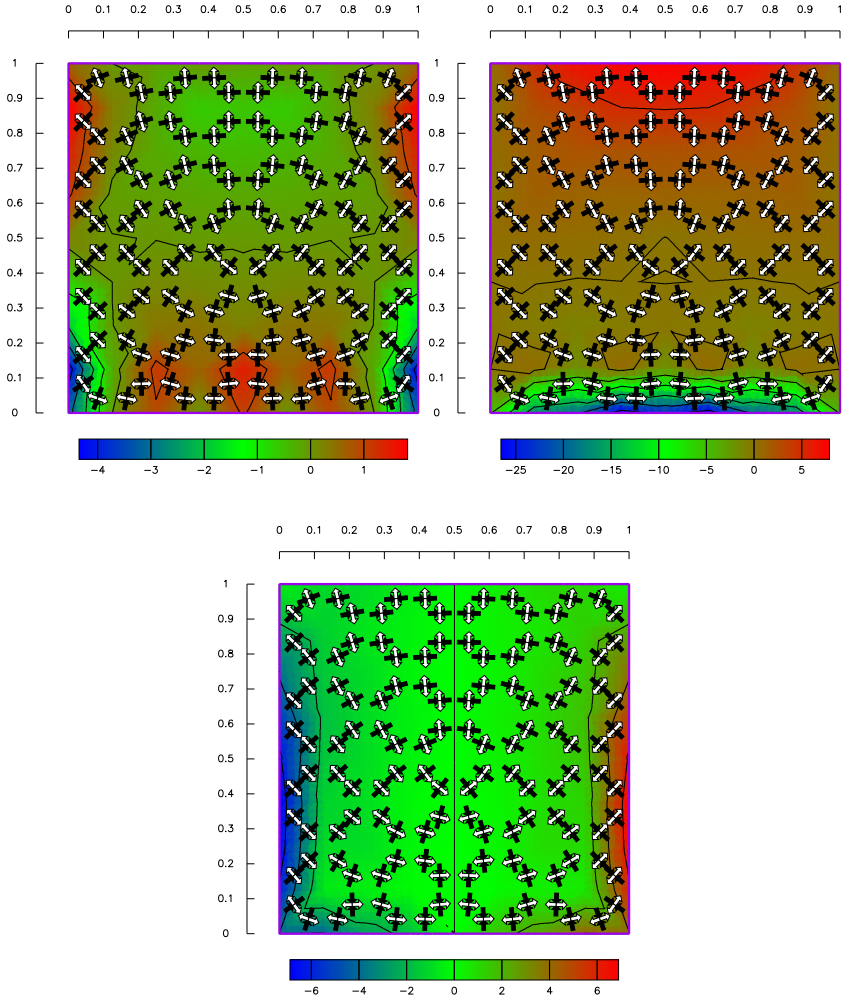

Figure II.24.: The strain-rate tensor components D_x, D_y, and D_{xy} (from left to right, from top to bottom) for the "locked up" ice ramp. 40 iterations, $a_{\max} = 0.01$.

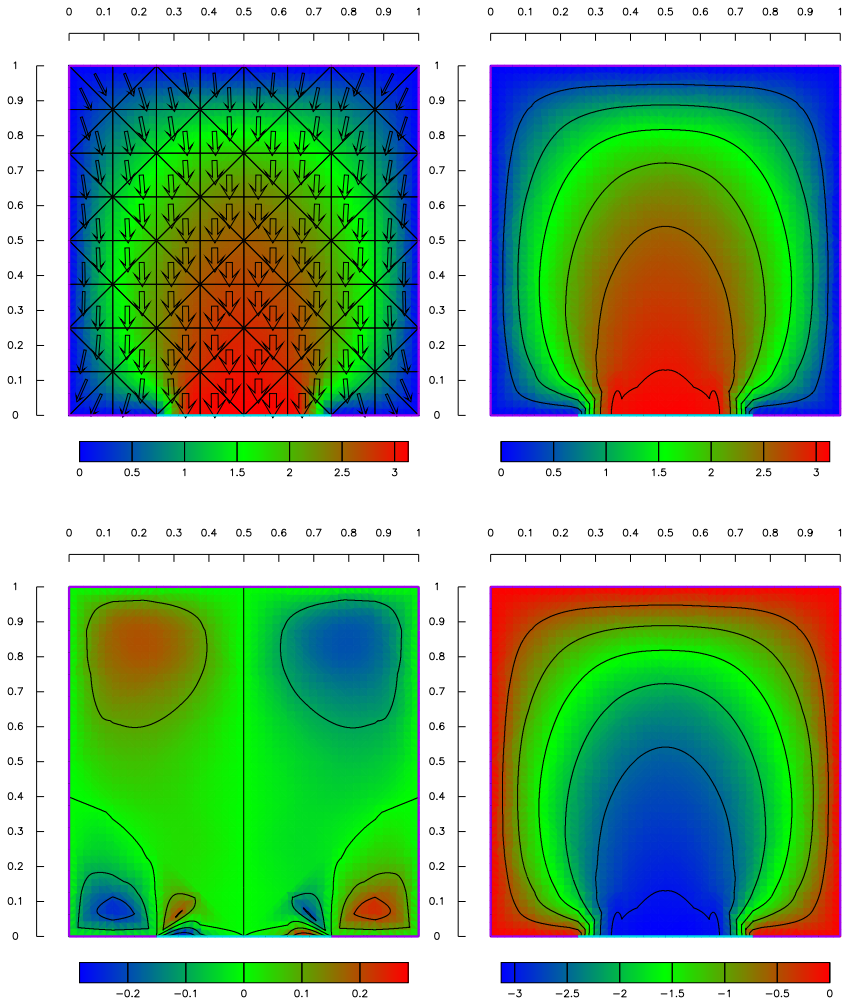

Figure II.25.: The velocity field together with the grid, v, v_x, and v_y (from left to right, from top to bottom) for the restricted calving front computation. 40 iterations, $a_{\max} = 0.01$.

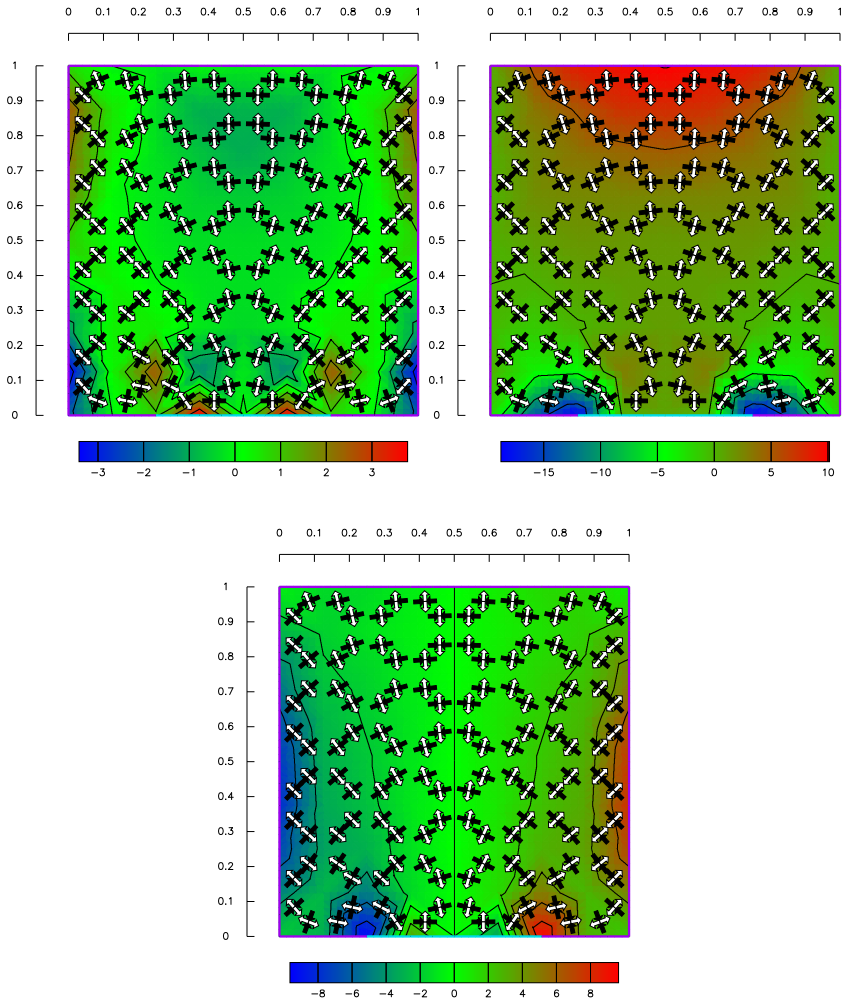

Figure II.26.: The strain-rate tensor components D_x, D_y, and D_{xy} (from left to right, from top to bottom) for the restricted calving front computation. 40 iterations, $a_{\max} = 0.01$.

II.3.2. Computations for the Ross Ice Shelf, Antarctica

After performing various calculations for different academic ice shelf setups, the numerical model shall now be applied to Antarctica's largest present ice shelf, the Ross Ice Shelf. Before this can be done, however, a dataset with all the geographical, topological and glaciological input quantities needed for running the model has to be assembled.
Around 1996, an international model intercomparison of different numerical ice-shelf models founded by the European Science Foundation was launched as part of the *European Ice Sheet Modeling Initiative* (EISMINT) program. For this work, a dataset for numerical modelling of the Ross Ice Shelf was assembled, c.f. MacAyeal et al. (1996). Unfortunately, however, this data is no longer available in digital form and could, therefore, not be used for this work: It is simply no longer trackable today, not even by the main author of the original publication (MacAyeal, personal communication). Therefore, all the data needed to set up a numerical model had to be assembled again from what was freely available, mainly over the Internet. The assembling of a new dataset for the numerical model was done in a joint effort together with a colleague, A. Humbert at the institute. It is mainly due to her work that a new dataset could be set up and that it can now be used to apply the numerical model to the Ross Ice Shelf.

The Ross Ice Shelf is located between 78°S to 86°S, 155°W to 160°W and it is named after James Clark Ross, a British polar explorer who first discovered this largest floating ice mass on Earth in 1841. Present area estimates range from 496,000 km^2 to 540,000 km^2, which is roughly the area of France. The location of the Ross Ice Shelf, together with that of the Filchner-Rønne and the Amery Ice Shelf is shown in figs II.27 and II.28. The main mass inflow into the Ross Ice Shelf originates from the large ice streams and huge glaciers flowing down from the Trasantarctic Mountains. The catchment areas of these glaciers as well as that of Ice Stream A lies mainly in the East Antarctic Ice Sheet, the other ice streams B, C, D, E and F as well as the Prestrud Inlet drain the West Antarctic Ice Sheet. There are mainly two regions, were the ice shelf runs aground and build up an ice rise: Crary Ice Rise and Roosevelt Island.

The ice streams are huge and fast flowing ice masses: Ice Stream B is 50 km wide where it becomes afloat, it is 800 m thick and its velocity exceeds 500 $\mathrm{m\,a}^{-1}$. Its discharge into the Ross Ice Shelf is more than 20 $\mathrm{km}^3\,\mathrm{a}^{-1}$, cf. Thomas et al. (1984). This is approximately the drainage

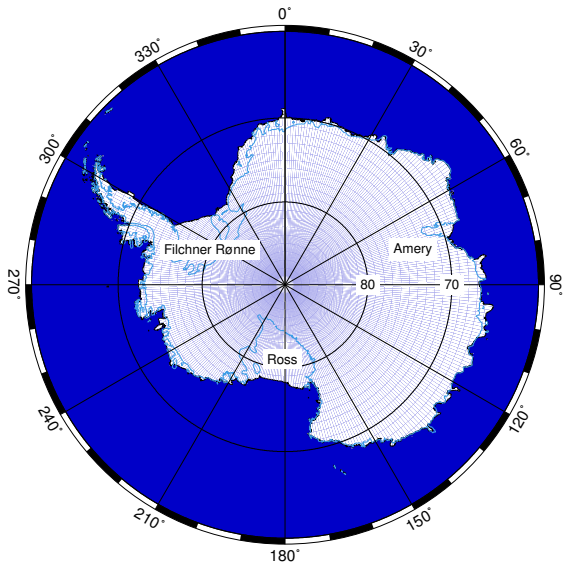

Figure II.27.: The location of the three major ice shelves.

of the seven major glaciers draining the East Antarctic Ice Sheet through the Transantarctic Mountains, not including Byrd Glacier. The ice streams are unique: Their flow behaviour is different from that of ice shelves and it is not comparable to the flow of ice sheets either; it can best be compared with the flow of fast moving, surging glaciers. Generally, it is assumed that their basal drag is substantially reduced by a lubricating layer composed of a mixture of sediment and water and that the velocity of the ice streams is determined by horizontal shear stresses at the lateral boundaries. Any change in the basal conditions has a significant impact on the flow properties of the ice stream. For example, Ice Stream E stopped approximately 150 a ago and according to Thomas et al. (1984), its present surface velocity is only slightly higher than the slow moving drainage of the adjacent Siple Dome. Nevertheless, the signature of Ice Stream E can still be clearly seen on satellite images. Most likely, the dynamics of the large ice streams is controlled by an unstable stick-slip condition at the base.

While deriving the theory that describes the dynamics of ice shelves in chapter I, incompressibility was one of the major assumptions made. Even though this is perfectly valid as far as the theoretical description of the flow properties of ice are concerned, this assumption must be partially

abandoned when assembling a dataset from measured values. This main problem that occurs is, that one can no longer adhere to the assumption of a vertically constant density profile when applying the floating condition to real world ice shelves. The lower density of the upper layers – where firn is transformed into ice - significantly influences the equilibrium position of the ice shelf. If one knew the density profile at any position on the ice shelf, a modified floating condition that takes the density variations into account, together with the ice surface topography and the ocean bathymetry, would ideally be suited for deriving the position of the grounding line. Unfortunately, the density profile, especially its changes from position to position all over the ice shelf, is a rather poorly known quantity. This problem is often addressed by deriving an empirical relation between the ice thickness and the surface topography of the ice shelf, e.g. Thyssen (1988), Shabtaie & Bentley (1982), Bamber & Bentley (1994). For certain regions, however, there are also direct measurements of the density profile from ice cores, e.g. Gerland et al. (1996).

During the assembling of the FE dataset for the Ross Ice Shelf, several sources were used: The ice thickness data as well as the water column underneath the ice shelf was taken from the BEDMAP project, 'BEDMAP Consortium' (2000) and the surface topography from the *Radarsat Antarctic Mapping Project Digital Elevation Model* (RAMP-DEM), Liu et al. (2000) is used; datasets for the surface velocity at different locations on the Ross Ice Shelf as well as along the ice streams and their catchment area were downloaded from the *National Snow and Ice Data Center* (NSIDC), cf. table II.6. The velocity data is completed by some values published in Thomas et al. (1984), that for some reason were not included in the NSIDC dataset.

It has to be pointed out clearly, that the dataset was assembled for one purpose only: for enabling an application of the numerical model to a real ice shelf. It is by no means a high quality data product and it is likely that it includes values that do not hold a comparison with real world data. A truly reliable dataset can only be assembled by an international collaboration that brings together modellers, data analysts and field people. Many of the limitations of the current data set are due to the limited resources that were available and the lacking access to the original measurements. For this reason, projects like BEDMAP, that try to bring together all the data that is already available today, are considered most valuable. In fact, such projects are essential for all theoretical and numerical modellers.

The following sketches how the dataset was assembled. The grounding line was extracted first using different methods. One approach utilized the floating condition to calculate where the ice is afloat and where not by using the ice thickness data from the BEDMAP project together with the surface topography from the RAMP-DEM. Since, however, the ice density distribution is only poorly known, the ice surface calculated from the floating condition differs largely from the RAMP-DEM data. Assuming a constant ice layering all over the ice shelf – this, however, is not necessarily realistic – the difference between the calculated and the actual surface from the RAMP-DEM should be constant wherever the ice is afloat. Furthermore, the transition from the inland ice to the ice shelf is characterized by a steep change in the surface slope and, therefore, the approximate position of the grounding line can usually be seen in satellite images. The further proceeding was to plot isolines for the difference between the ice surface calculated from the floating condition and the topography from the RAMP-DEM. That isoline, that matched best with the satellite image was chosen as a first estimate of the position of the grounding line.

The second approach was to derive the grounding line as the zero isoline of the water column beneath the ice shelf. Even though this seems to be convincingly simple, it does not necessarily lead to meaningful results. This is because the water column is only measured at certain locations, and definitely not along the whole grounding line*. The dataset, however, gives a certain value for the water column at any grid point. Presumably due to the interpolation, there are locations where there is a non-zero water column but the ice thickness vanishes, especially on the side of the Transantarctic Mountains.

Despite the limited accuracy of both methods, the results were combined and used as a first approximation for the position of the grounding line. The accuracy of the grounding-line position certainly influences the results obtained from numerical modelling. There are, however, other quantities like the ice thickness, the surface velocity and the mass influx† that have to be prescribed as well, and these quantities are also not avail-

*Only the water column at the grid points of the BEDMAP dataset were available for this work, but not the original locations where it was actually measured; not even the number of measured values were known.

†Even though the horizontal velocities are vertically constant in the SSA limit, this is not necessarily true at the grounding line where inlets enter the ice shelf. Depending on the basal conditions, glaciers are likely to have a strong velocity profile.

able at a very high level of accuracy. Since the SSA equations do not hold at the grounding line anyhow, it is better to shift the points of the model grounding line towards the centre of the ice shelf in case there is any inconsistency in the datasets. Therefore, the final decision on which points are used to define the planar straight line graph (PSLG) of the grounding line for the numerical model was done by hand using the following criteria:

- The grounding line should approximately match the position that can be estimated from the satellite picture.
- The points of the PSLG should have meaningful ice thicknesses in the BEDMAP data. If not, they are moved further inwards into the ice shelf.
- Any of the inlets should be represented by at least three points, one on each side and one in the middle. Ice Streams A and B as well as D and E are modelled as combined ice streams.
- The extent of the inlets as well as the flow direction is estimated from the satellite image.

Once the grounding line was fixed, a grid with a certain area constraint was generated and the ice thickness was interpolated linearly from the BEDMAP grid onto the node positions. Finally, the velocity boundary conditions were prescribed: Along the two ice rises and in between the inlets, a zero velocity condition is used. For several reasons, it is not sufficient to prescribe measured surface velocity data for the inlets. This would lead to unrealistic volume fluxes. One reason for this is issued from using second order polynomials for the FE method: The position of the inlets is prescribed by at least three nodes, i.e. each of the inlets is represented by at least two boundary segments in the PSLG. Using second order polynomials, however, introduces an additional node on each of the boundary segments. Since these nodes shall be generated automatically, some interpolation has to be used to compute reasonable values for the velocity at the position of the new nodes (linear interpolation is used for this). This, however, has an influence on the velocity profile along a cross-section of the inlet. Furthermore, depending on where exactly the surface velocities were measured on the glaciers and ice streams, the values may not be representative for the whole ice thickness of the inlet since it depends on the basal conditions whether the inlets do have a vertical velocity profile or

not. The numerical model is based on the SSA equations and, therefore, it implicitly assumes that the horizontal velocities are vertically constant. All this leads to unrealistic volume fluxes if measured values of the horizontal velocities are used as the velocity boundary condition. Therefore, the following approach was used: The absolute values of the velocity were first chosen according to measured data (see table II.7) or were just estimated where no data was available. Then, the numerical grid was generated and the volume fluxes were computed. As long as unrealistic values were obtained, the velocities were adjusted and the procedure was repeated again. The finally obtained volume fluxes are summarized in table II.8. The upper graph of fig. II.29 shows the model grounding line and the inlets mapped on a AVHRR satellite picture obtained from http://terraweb.wr.usgs.gov.

region	*related publication*
central part of the Ross Ice Shelf	Thomas et al. (1984), data obtained from the *Ross Ice Shelf Geophysical and Glaciological Survey, RIGGS*
north west region	Scambos et al. (1992)
Ice Stream D, E	Bindschadler et al. (1996)
Ice Stream B	Whillans & Van der Veen (1993)
lower part of Ice Stream D	Scambos et al. (1992)
Prestrud Inlet	Scambos et al. (1992)
Siple Dome	Nereson (1998)
catchment area of Ice Stream B, C, D and E	Whillans & Van der Veen (1993)

Table II.6.: Original publications of the velocity data used. The datasets can be downloaded from the *National Snow and Ice Data Center* (NSIDC), http://nsidc.org/NSIDC/ANTARCT_VELOC.

A reasonable agreement between the computed velocities and measured values is obtained using a rate factor of $7.23 \cdot 10^{-17}\,\mathrm{kPa\,s^{-1}}$, what approxi-

ice stream / glacier	*volume flux* $[\mathrm{km^3\,a^{-1}}]$	*velocity* $[\mathrm{m\,a^{-1}}]$	*references*
Ice Stream F	1.3	200	MacAyeal & Thomas (1986)
	5.7±0.9		Shabtaie & Bentley (1987)
Ice Stream E	20.8	650	MacAyeal & Thomas (1986)
	> 24		Thomas et al. (1984)
	25.1±2.3		Shabtaie & Bentley (1987)
Ice Stream D	9.7	550	MacAyeal & Thomas (1986)
	≈ 10		Thomas et al. (1984)
	21.5±1.8		Shabtaie & Bentley (1987)
Ice Stream C	3.9	150	MacAyeal & Thomas (1986)
	0.4±0.2		Shabtaie & Bentley (1987)
Ice Stream B	25.5	750	MacAyeal & Thomas (1986)
	> 20	> 500	Thomas et al. (1984)
	26.6±3.1		Shabtaie & Bentley (1987)
Ice Stream A	6.3	225	MacAyeal & Thomas (1986)
	12.6±1.1		Shabtaie & Bentley (1987)
Scott Glacier	1.9	170	MacAyeal & Thomas (1986)
Amundson Glacier	1.9	170	MacAyeal & Thomas (1986)
Liv Glacier	1.6	230	MacAyeal & Thomas (1986)
Shackleton Glacier	0.9	170	MacAyeal & Thomas (1986)
Beardmore Glacier	8.5	470	MacAyeal & Thomas (1986)
Nimrod Glacier	2.7	250	MacAyeal & Thomas (1986)
Byrd Glacier	14	600	MacAyeal & Thomas (1986)
	18	> 800	Thomas et al. (1984)
Mulock Glacier	2.8	285	MacAyeal & Thomas (1986)

Table II.7.: Volume flux and surface velocity data used to assemble the FE dataset.

ice stream / glacier	*volume flux* $[\mathrm{km}^3\,\mathrm{a}^{-1}]$
Prestrud Inlet	1.85
Ice Stream F	6.16
Ice Stream E and D	38.11
Ice Stream B and A	33.9
Scott Glacier	2.01
Amundson Glacier	1.9
Liv Glacier	0.55
Shackleton Glacier	0.99
Beardmore Glacier	3.99
Nimrod Glacier	1.84
Byrd Glacier	16.93
Darwin Glacier	1.03
Mulock Glacier	2.1
Skelton Glacier	1.34

Table II.8.: Volume fluxes used in the numerical model.

mately corresponds to an ice temperature of $-27°C$, cf. table B.1(b). This might be somewhat too cold for the entire ice shelf, but it is not completely unrealistic compared to the temperature profiles given in Paterson (1994). Figs II.30 shows the computed velocity field after 30 iterations ($w = 0.8$). The arrows provide a good visualisation of the flow around Crary Ice Rise and Roosevelt Island. It should be stressed again, that they are attached to the centres of mass of the triangles and that they scale with the absolute velocity. There is no outflow out of ice-shelf domain except at the calving front. Figs II.30 together with figs II.31 already show what will be confirmed by a comparison with measured velocity data: The inflow from the ice streams does not have a significant impact on the overall flow field in the computation. The upper graph of figs II.32 shows again the computed velocities in $\mathrm{m\,a^{-1}}$ and can directly be compared with the lower one showing the measured surface velocities. In this graph, the locations of the measurements are marked with white crosses. By and large, the agreement is satisfactory, especially in the frontal zone not too far away from the calving front. The numerical model, however, has an obvious problem with the inflow from the ice streams: The "green tongues" towards Ice Stream D, E and A, B are not reproduced by the numerical computation. The same holds for the region near the mouth of the Byrd Glacier. Increasing the temperature, it is well possible to improve the results for the ice streams, but at the cost of a much too high velocity at the calving front. These results are in agreement with MacAyeal & Thomas (1982) who also obtained a too high velocity near the calving front and much too low velocities near the grounding line. The explanation given by the authors can, however, not be confirmed: It is argued that the discrepancy between the numerical results and the measured values is mainly due to problems with the numerical convergence of the model. As it can be seen from fig. II.33(b), this is definitely not the case here. Fig. II.33(a) shows the difference between the numerical computation and the measured values. It again unveils the strong and the weak points of the numerical solution.

Unfortunately, there is no really convincing argument that could explain why the numerical model cannot adequately reproduce the inflow regions of the ice streams. Since, however, this model is not the only one that shows this behaviour, several questions may be raised: Is the ice closer to the ice streams somehow softer? If so, why? Is it due to the temperature, due to anisotropy or due to a weakening caused by crevasses at the surface? It should, however, be kept in mind that at present, the numerical model

as well as the data set both do have certain limitations and, therefore, the results should not be over-interpreted. At this stage, the numerical model is only a diagnostic tool since it can only compute the velocity field for a given setup. A first extension towards a prognostic tool would be to implement the evolution equations formulated in the theoretical part of this work. Another weakness of both, the present theoretical description as well as the numerical implementation certainly is the treatment of the boundary condition along the ice rises. Even the second order equations as derived by Baral (2000) do not show how the transition zone where the ice shelf becomes afloat can be incorporated into the numerical model. It is likely that some kind of parameterisation has to be used here, but this is still ongoing research.

The following two main conclusions can be drawn from applying the numerical model to both, academic ice-shelf setups and to the Ross Ice Shelf:

- In principle, the model is applicable to real world ice shelves.
- In order to obtain meaningful results, a reliable data set is necessary. The one presented can only be a first step in that direction. An international collaboration that brings together the data already available today is necessary for that. BEDMAP is very valuable in this regard, but it is only a first step in that direction.